Complete FDTD Analysis of Microwave Heating Processes in Frequency-Dependent and Temperature-Dependent Media

François Torres and Bernard Jecko

***Abstract*— It is well known that the temperature rise in a material modifies its physical properties and, particularly, its dielectric permittivity. The dissipated electromagnetic power involved in microwave heating processes depending on $\varepsilon(\omega)$, the electrical characteristics of the heated media must vary with the temperature to achieve realistic simulations. In this paper, we present a fast and accurate algorithm allowing, through a combined electromagnetic and thermal procedure, to take into account the influence of the temperature on the electrical properties of materials. First, the temperature dependence of the complex permittivity ruled by a Debye relaxation equation is investigated, and a realistic model is proposed and validated. Then, a frequency-dependent finite-differences time-domain ($(FD)^2TD$) method is used to assess the instantaneous electromagnetic power lost by dielectric hysteresis. Within the same iteration, a time-scaled form of the heat transfer equation allows one to calculate the temperature distribution in the heated medium and then to correct the dielectric properties of the material using the proposed model. These new characteristics will be taken into account by the EM solver at the next iteration. This combined algorithm allows a significant reduction of computation time. An application to a microwave oven is proposed.**

I. Introduction

HEATING applications of microwaves have been widely investigated in recent years [1], and a lot of experimental and theoretical work has been carried out, both in medical [2]–[5] and industrial [6]–[10] domains. From the theoretical point of view, realistic models have been developed through computer simulations to determine the temperature distribution induced by microwave radiation in complicated structures of arbitrary shapes. The thermal problem is treated by solving the heat transport equation (HTE) [3], [7], [8], [11]–[14] to obtain the heating patterns. This heat transport equation involves a term related to the dissipated electromagnetic power, which can be assessed by many numerical methods. A review of numerical models used for medical purposes has been given by Spiegel [15], who stated that the finite-difference time-domain (FDTD) method is finding an increased usage for the electromagnetic and thermal resolution of such problems.

The electromagnetic power dissipation leading to heat generation is due to dielectric and conduction losses in the heated media, and consequently a knowledge of the dielectric and conduction properties of materials is imperative to achieve realistic simulations. In early work using FDTD method [3], [16]–[18], computations were performed assuming monochromatic or narrow frequency bandwidth waves, and, therefore, supposed constant real permittivities and constant equivalent conductivities including both dielectric and conduction losses at the frequency of interest. These assumptions were due to the inability of the FDTD method to take the frequency dependence of dielectric properties into account. This weak point of the FDTD algorithm has been overcome in recent works [19]–[22], which present time-domain formulations allowing for the FDTD resolution of problems for media for which the complex permittivity $\varepsilon(\omega)$ may be described by a Debye or Lorentz equation. Generally, the media complex permittivities at microwave frequencies can be fitted by the Debye relaxation equation, and this formulation has been used in recent applications [5], [21], [22] with a good agreement between theory and experimentation.

In most cases [3], [5], where constant or frequency-dependent permittivities are used, the heating patterns are computed once the electromagnetic problem is solved and the electromagnetic power density in the media is known. However, it is well known that the temperature elevation inside a medium leads to changes in its physical properties, and especially modifies the complex permittivity of the medium. As a result, the dissipated power, which depends on this quantity, becomes temperature-dependent. If this fact is not taken into account, the computed electromagnetic fields distribution in the medium can be erroneous, with a resulting overestimation of the temperature.

In a recent work [8], Ma *et al*. have proposed a combined electromagnetic and thermal FDTD model, allowing to take the temperature dependence of the electrical properties of the heated media into account during the electromagnetic resolution, but the time steps used in the two algorithms remained very different: close to 1 ps for the electromagnetics and close to 1 s for the thermal. Thus, the authors have adopted the following approach: the electromagnetic solver is run until the steady state is reached, and then the power dissipation distribution is computed from the root mean square (rms) value of the electric field monitored over a period of the incident frequency. The temperature distribution is then computed during a few time steps of the thermal algorithm and used to update the electrical properties of the medium. The electromagnetic resolution is then resumed, taking into

Manuscript received August 15, 1996; revised September 23, 1996.

The authors are with the Institut de Recherche en Communications Optiques et Microondes (I.R.C.O.M.), Université de Limoges, 87060 Limoges Cedex, France.

Publisher Item Identifier S 0018-9480(97)00273-1.

account these new characteristics. Once the steady state is reached again, the above procedure is repeated until the actual heating time is reached. The drawback of such a method is to require large computation times (the authors mention 12 h on an HP730 workstation for the case of a microwave oven).

This paper presents a way to speed up such a procedure within the same FDTD algorithm, through the direct determination of the temperature distribution in frequency-dependent materials, for which a temperature-dependent Debye relaxation equation is assumed for the description of the permittivity. In Section II, the temperature dependence of the parameters involved in the permittivity of a Debye medium is investigated and a realistic model is proposed and validated by a comparison with measurement results. As the dielectric properties of the media have to be modified by the heating effects of electromagnetic waves, a time-domain formulation of the electromagnetic power dissipated by dielectric hysteresis is presented in Section III and is used as a source term in the heat transport equation developed in Section IV. At this point, time scaling problems between Fourier's and Maxwell's equations are pointed out, and a way to overcome such problems is presented and validated. Finally, some applications are studied in Section V and, in particular, the heating phenomena inside a microwave oven are presented.

II. Temperature Dependence of the Complex Debye Permittivity

The classical theory for polar liquids is due to Debye [23], but it can be more generally used to characterize a medium containing microscopic permanent or induced dipoles, whose macroscopic resultant is known as the polarization of the medium. This polarization $\vec{P}(\omega)$ is linked to the macroscopic electric field $\vec{E}(\omega)$ through the medium's relative susceptibility $\chi(\omega)$ or the relative permittivity $\varepsilon(\omega)$ by the relation:

$$\vec{P}(\omega) = \varepsilon_0 \chi(\omega) \vec{E}(\omega) \tag{1}$$

or

$$\vec{P}(\omega) = \varepsilon_0 (\varepsilon(\omega) - \varepsilon_\infty) \vec{E}(\omega) \tag{2}$$

where the complex relative permittivity $\varepsilon(\omega)$ can be described by the first-order equation:

$$\varepsilon(\omega) = \varepsilon_\infty + \frac{\varepsilon_s - \varepsilon_\infty}{1 + j\omega\tau}. \tag{3}$$

Here ε_∞ is the infinite frequency relative permittivity, ε_s the static relative permittivity, and τ the relaxation time. We shall here limit the developments to a single relaxation time medium, but the generalization to media characterized by several relaxation times and static permittivities, as now used in [5], [22], can be easily made.

A lot of work has been done [23]–[28] to precisely define the different quantities of (3), and it has been shown [24]–[28] that only the temperature dependence of the static permittivity and the relaxation time have to be considered to achieve a good agreement between theoretical models and measured data. The variations of the infinite permittivity with the temperature are quite negligible compared to the other variations.

A. Static Permittivity

Several models have been developed to analytically determine the static permittivity [24], [25], and they basically differ in the assumptions used to evaluate the local electric field, which is the microscopic field acting on one dipole. The Clausius–Mosotti formula [24], based on the original treatment of the local field established by Lorentz [29], leads to erroneous values for the static permittivity in some cases [28]. This model has been improved by Onsager [30], and it gives quite a good approximation of ε_s. Further refinements of the Onsager theory have been established by Kirkwood [28], but they require additional parameters that are not easily available for all dielectrics.

Therefore, we decided to use the Onsager model for the determination of the temperature dependence of ε_s. This model leads to the following static formula [26]:

$$\frac{3(\varepsilon_s - \varepsilon_\infty)(2\varepsilon_s + \varepsilon_\infty)}{\varepsilon_s(\varepsilon_\infty + 2)^2} T = N \frac{p_m^2}{3\varepsilon_0 k} \tag{4}$$

where p_m is the moment of a single dipole, N the number of dipoles per unit volume, k the Boltzmann's constant, and T the temperature. The right-hand term of (4) has to be estimated from measured data for the considered dielectric, and in order to achieve the best agreement with experimental data, the dipole density N is taken to be temperature-dependent and we use the Boltzmann's statistics [32] to represent this behavior:

$$N = N_0 \exp(-U/kT) \tag{5}$$

where U is the potential energy of a dipole and N_0 is a constant of the medium. Since the other quantities of the right-hand term of (4) are independent of the temperature, (4) can be written as

$$\frac{3(\varepsilon_s - \varepsilon_\infty)(2\varepsilon_s + \varepsilon_\infty)}{\varepsilon_s(\varepsilon_\infty + 2)^2} T = A_0 \exp(-U/kT) \quad \text{with } A_0 = N_0 \frac{p_m^2}{3\varepsilon_0 k}. \tag{6}$$

However, the values of A_0 and U are generally unavailable for all media, but they can be easily deduced from a couple of experimental data.

A knowledge of these values allows one to develop (6) as a classical second-order equation, whose positive root gives the analytical temperature dependence of ε_s, shown in (7) at the bottom of this page.

$$\varepsilon_s(T) = \frac{3\varepsilon_\infty T + A(\varepsilon_\infty + 2)^2 + \sqrt{(3\varepsilon_\infty T + A(\varepsilon_\infty + 2)^2)^2 + 72\varepsilon_\infty^2 T^2}}{12T} \qquad \text{with } A = A_0 \exp(-U/kT). \tag{7}$$

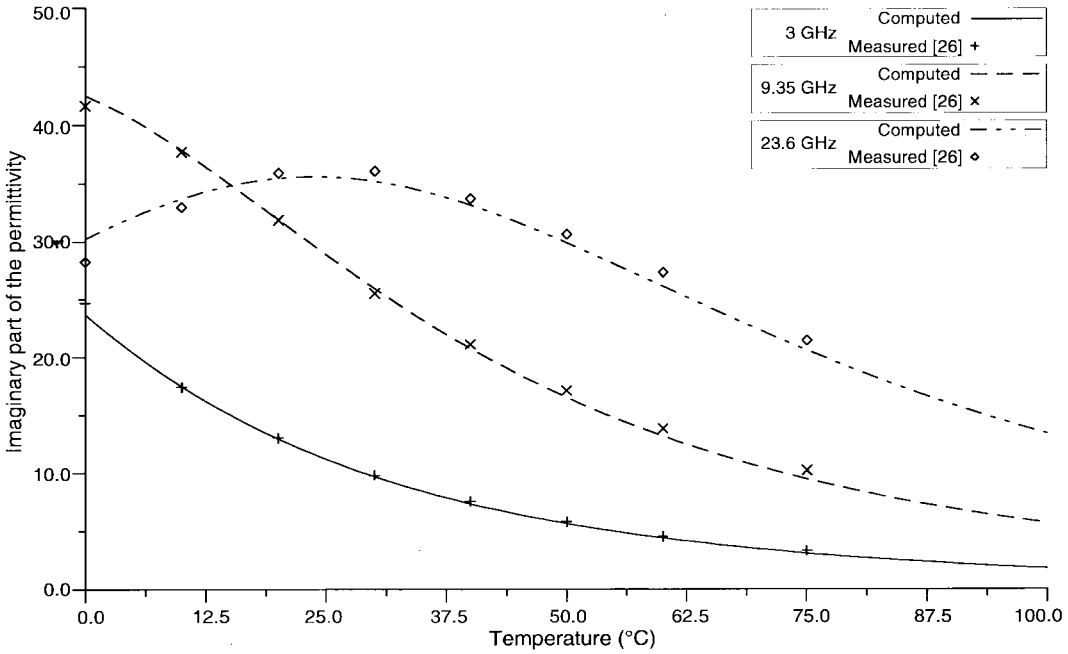

Fig. 1. Computed and measured temperature dependence of the imaginary part of the water permittivity.

B. Relaxation Time

The macroscopic relaxation time used in (3) is not the same as the molecular relaxation time defined by Debye, differing from it by a constant factor that depends on the theory assumed for the static permittivity. Moreover, the basic physical processes involved in the relaxation phenomena are not the same for liquids and solids [24]. However, the analytical law ruling the temperature dependence of the macroscopic relaxation time happens to have the same form for liquids and solids [25], [31]:

$$\tau = \tau_0 \exp(W_a/kT) \tag{8}$$

where k is Boltzmann's constant, T the temperature, τ_0 a constant of the medium, and W_a is generally known as the activation energy, which refers in liquids to an energy connected to the viscosity and in solids to the height of the energy barrier between equilibrium positions of the dipoles. The values of τ_0 and W_a are not available for all media, but, as for the static permittivity, can be deduced from a couple of experimental data giving the temperature dependence of the complex permittivity.

To validate this model, water has been taken as an example. This polar dielectric has been extensively investigated, and data on its complex permittivity are easily available [26]. Assuming $\varepsilon_\infty = 5.5$, the following values have been found from experimental data:

$$W_a = 2.96\ 10^{-20}\ \text{J}$$
$$\tau_0 = 6.27\ 10^{-15}\ \text{s}$$
$$U = -2.88\ 10^{-21}\text{J}$$

and

$$A_0 = 1186.78.$$

Using these values, the temperature dependence of the static permittivity and relaxation time have been computed and the imaginary part of the complex permittivity has been determined for three microwave frequencies for which measurements are available [26] (3, 9.35, and 23.6 GHz). Results are plotted on Fig. 1, which shows a good agreement between the experimental points and the simple model we used.

III. Dissipated Power

In order to assess the temperature evolution inside a dispersive dielectric medium, it is necessary to evaluate the dissipated power in the material. In most applications, the FDTD electromagnetic solver is run to compute the sinusoidal steady-state fields, then the dissipated power deposition and the heating patterns are determined in the medium. As the temperature dependence of the complex permittivity has to be taken into account, the dissipated power and the temperature distribution must be computed during the electromagnetic resolution whatever the time-domain evolution of the incident wave is. Therefore, the classical expression for the mean power lost by dielectric hysteresis, i.e.,

$$\overline{P_d(\omega)} = \frac{1}{2}\varepsilon_0 \omega \varepsilon''(\omega)|E|^2 \tag{9}$$

is no longer valid since it is restricted to steady-state time-harmonic electromagnetic fields, and consequently the dissipated power has to be expressed in the time domain.

In its local form, the energy conservation equation is

$$\text{div}\vec{S} + \frac{\partial \rho_w}{\partial t} = -P \tag{10}$$

where

$\vec{S}$ Poynting's vector $\vec{S} = \vec{E} \times \vec{H}$;
P power dissipated per unit volume;
ρ_w volumic energy density, which can be written as

$$\rho_w = \frac{1}{2}(\vec{E} \cdot \vec{D} + \vec{H} \cdot \vec{B}). \tag{11}$$

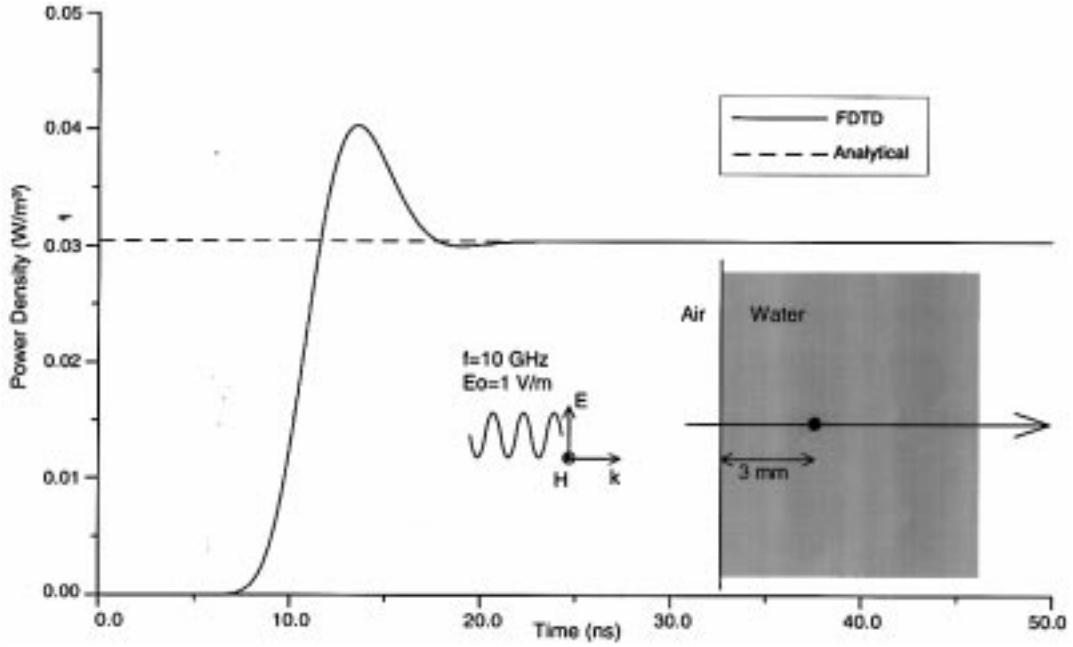

Fig. 2. Comparison between the FDTD expression for the power lost by dielectric hysteresis (16), and the analytical value (9).

The classical expression of the divergence of a cross product leads to

$$\mathrm{div}(\vec{E}\times\vec{H}) = \vec{H}\cdot\mathrm{curl}\vec{E} - \vec{E}\cdot\mathrm{curl}\vec{H}. \tag{12}$$

Using Maxwell's curl equations

$$\mathrm{curl}\vec{E} = -\frac{\partial\vec{B}}{\partial t} \tag{13}$$

and

$$\mathrm{curl}\vec{H} = \frac{\partial\vec{D}}{\partial t} + \vec{j} \tag{14}$$

and identifying the terms involved in the time derivative of ρ_w, (12) can be written as

$$\mathrm{div}(\vec{E}\times\vec{H}) + \frac{\partial\rho_w}{\partial t} = -\frac{1}{2}\left(\vec{E}\cdot\frac{\partial\vec{D}}{\partial t} - \vec{D}\cdot\frac{\partial\vec{E}}{\partial t}\right) - \frac{1}{2}\left(\vec{H}\cdot\frac{\partial\vec{B}}{\partial t} - \vec{B}\frac{\partial\vec{H}}{\partial t}\right) - \vec{j}\cdot\vec{E}. \tag{15}$$

As in (10), the second term of (15) is the total power dissipated per unit volume and can be more distinctly identified as

$$P_e = \frac{1}{2}\left(\vec{E}\cdot\frac{\partial\vec{D}}{\partial t} - \vec{D}\cdot\frac{\partial\vec{E}}{\partial t}\right) \tag{16}$$

which is the instantaneous power dissipated by dielectric hysteresis per unit volume:

$$P_m = \frac{1}{2}\left(\vec{H}\cdot\frac{\partial\vec{B}}{\partial t} - \vec{B}\cdot\frac{\partial\vec{H}}{\partial t}\right) \tag{17}$$

which is the instantaneous power dissipated by magnetic losses per unit volume, and

$$P_j = \vec{j}\cdot\vec{E} \tag{18}$$

which is the instantaneous power dissipated by conduction losses per unit volume.

Assuming a nonmagnetic and nonconductive medium, the power dissipated per unit volume reduces to the dielectric hysteresis losses:

$$P_d = P_e = \frac{1}{2}\left(\vec{E}\cdot\frac{\partial\vec{D}}{\partial t} - \vec{D}\cdot\frac{\partial\vec{E}}{\partial t}\right). \tag{19}$$

To be used as a source term for the thermal algorithm, the power dissipated per unit volume is evaluated at the center of every FDTD cell containing a dissipative medium, using the spatial average value of each $\vec{E}$ and $\vec{D}$ field component.

In order to demonstrate the validity of the dissipated power expression (16), a one-dimensional finite-difference computation has been performed considering a plane wave normally incident at a planar interface between air and a temperature-independent dispersive Debye medium characterized by $\varepsilon_s = 76.4$, $\varepsilon_\infty = 5.5$, and $\tau = 8$ ps and modeled using the frequency-dependent finite-differences time-domain ($(FD)^2TD$) formalism of [22]. The incident field is a sinusoidal wave at the frequency of 10 GHz with an electric field amplitude of 1 V/m. The cell size is 0.1 mm and the time step is 0.16 ps. The dissipated power is computed in the medium at 3 mm beneath the interface using (16). Shown in Fig. 2 is a comparison of the time-domain computation and the exact value obtained with the analytical expression (9). An excellent agreement is found once the electromagnetic fields in the medium have reached the sinusoidal steady state. Moreover, an analytical confirmation of this result can be obtained. By assuming in expression (16) a time-harmonic dependence of the electromagnetic field, and using the frequency-domain relation $\vec{D}(\omega) = \varepsilon_0\varepsilon(\omega)\vec{E}(\omega)$, the classical expression (9) of the mean dissipated power can be established.

IV. Heating Patterns Determination

The electromagnetic-induced heating pattern in a medium exposed to an electromagnetic field may be obtained from the heat transport equation (HTE), also known as the Fourier's equation. In the presence of a cooling fluid circulating inside the medium, this equation is

$$\rho_m C_m \frac{\partial T(x,y,z,t)}{\partial t} = k_t \nabla^2 T(x,y,z,t) - V_s(T(x,y,z,t) - T_a) + P_d(x,y,z,t) \tag{20}$$

where

ρ_m	medium density ($\mathrm{kg \cdot m^{-3}}$);
C_m	specific heat of the medium ($\mathrm{J \cdot K^{-1} \cdot kg^{-1}}$);
k_t	thermal conductivity of the medium ($\mathrm{W \cdot m^{-1} \cdot K^{-1}}$);
$T(x,y,z,t)$	medium temperature (K);
V_s	product of flow and heat capacity of the cooling fluid ($\mathrm{W \cdot m^{-3} \cdot K^{-1}}$);
T_a	temperature of the cooling fluid (K);
$P_d(x,y,z,t)$	electromagnetic power dissipated per unit volume ($\mathrm{W \cdot m^{-3}}$).

For simplicity in solving this equation, the parameters ρ_m, C_m, and k_t are taken to be independent of position, temperature, and time.

At this point, attention must be paid to the time scales: in realistic cases, the heating process extends over seconds or minutes, strongly depending on the incident power, while the electromagnetic steady-state is reached in a few nanoseconds at microwave frequencies. This time scaling problem can be overcome in a simple way: Rewriting (20) as

$$\frac{\partial T}{\partial t} = \frac{k_t}{\rho_m C_m}\left(\frac{\partial^2 T}{\partial x^2} + \frac{\partial^2 T}{\partial y^2} + \frac{\partial^2 T}{\partial z^2}\right) - \frac{V_s}{\rho_m C_m}(T - T_a) + \frac{P_d}{\rho_m C_m} \tag{21}$$

and multiplying it by a constant factor α leads to

$$\alpha\frac{\partial T}{\partial t} = \frac{\alpha k_t}{\rho_m C_m}\left(\frac{\partial^2 T}{\partial x^2} + \frac{\partial^2 T}{\partial y^2} + \frac{\partial^2 T}{\partial z^2}\right) - \frac{\alpha V_s}{\rho_m C_m}(T - T_a) + \frac{\alpha P_d}{\rho_m C_m}. \tag{22}$$

From this equation, it can be seen that if the dissipated power P_d, the thermal conductivity k_t, and the cooling factor V_s are multiplied by α, the temperature evolution ($\partial T/\partial t$) is α times quicker, while its spatial evolution remains the same. Introducing the thermal diffusivity D_t as

$$D_t = \frac{k_t}{\rho_m C_m} \tag{23}$$

(22) can be written as

$$\alpha\frac{\partial T}{\partial t} = \alpha D_t\left[\left(\frac{\partial^2 T}{\partial x^2} + \frac{\partial^2 T}{\partial y^2} + \frac{\partial^2 T}{\partial z^2}\right) - \frac{V_s}{k_t}(T - T_a) + \frac{P_d}{k_t}\right]. \tag{24}$$

In other words, when the thermal diffusivity D_t is multiplied by α, the temperature evolution, given by (24), is α times quicker. The scaling effects on the dissipated power P_d, on the thermal conductivity k_t, and on the cooling factor V_s are implicitly expressed in (24). Therefore, it is possible to scale the heating time down to the duration of the FDTD EM computation, but obviously, the FDTD time window must be large enough to reach the steady state in the studied medium, including the possible resonances of the limited structures, and the heating process must be started only once this steady state is established. The way to set the parameters to fit the computation time window is quite simple and is summarized below.

Suppose we want to scale an actual heating duration T_{heat} to the EM computation time window T_{FDTD}, the scaling factor α is

$$\alpha = T_{\mathrm{heat}}/T_{\mathrm{FDTD}} \tag{25}$$

and the thermal diffusivity is to be simply multiplied by α to achieve this time scaling. Once the computation is over, the temperature evolution over the actual heating duration can be simply obtained by multiplying the FDTD time by the scaling factor α.

Considering this fact, Fourier's equation can be easily solved, and several implicit finite-difference schemes have been proposed [3], [5], [7], but, as in [8], we used the classical explicit algorithm for simplicity, and, if no cooling effects are assumed, it leads to the following equation in a three-dimensional case:

$$\begin{aligned} T^{n+1}(i,j,k) &= T^n(i,j,k) + \Delta t \alpha D_t \\ &\times \left[\frac{T^n(i+1,j,k) - 2T^n(i,j,k) + T^n(i-1,j,k)}{\Delta x^2} \right. \\ &+ \frac{T^n(i,j+1,k) - 2T^n(i,j,k) + T^n(i,j-1,k)}{\Delta y^2} \\ &+ \frac{T^n(i,j,k+1) - 2T^n(i,j,k) + T^n(i,j,k-1)}{\Delta z^2} \\ &\left. + \frac{P_d^n(i,j,k)}{k_t}\right] \end{aligned} \tag{26}$$

and the FDTD grid used to solve Maxwell's equations can be used for the resolution of (26). Thus, the time and space increments ($\Delta t, \Delta x, \Delta y$ and Δz) are the same as those used by the FDTD EM solver. As for the dissipated power, the temperature nodes are located at the center of every FDTD cell.

The stability criterion of (26), i.e.,

$$\Delta t \le \frac{1}{2\alpha D_t}\left(\frac{1}{\Delta x^2} + \frac{1}{\Delta y^2} + \frac{1}{\Delta z^2}\right)^{-1} \tag{27}$$

is generally less restricting than the classical stability condition used for the electromagnetic fields FDTD resolution [33]. But, due to the large values the scaling factor α can reach, the time increment needed to ensure the stability of (26) must be compared to the classical FDTD time step [33], and the smallest value must be chosen for both Maxwell's and heat transport equations resolution.

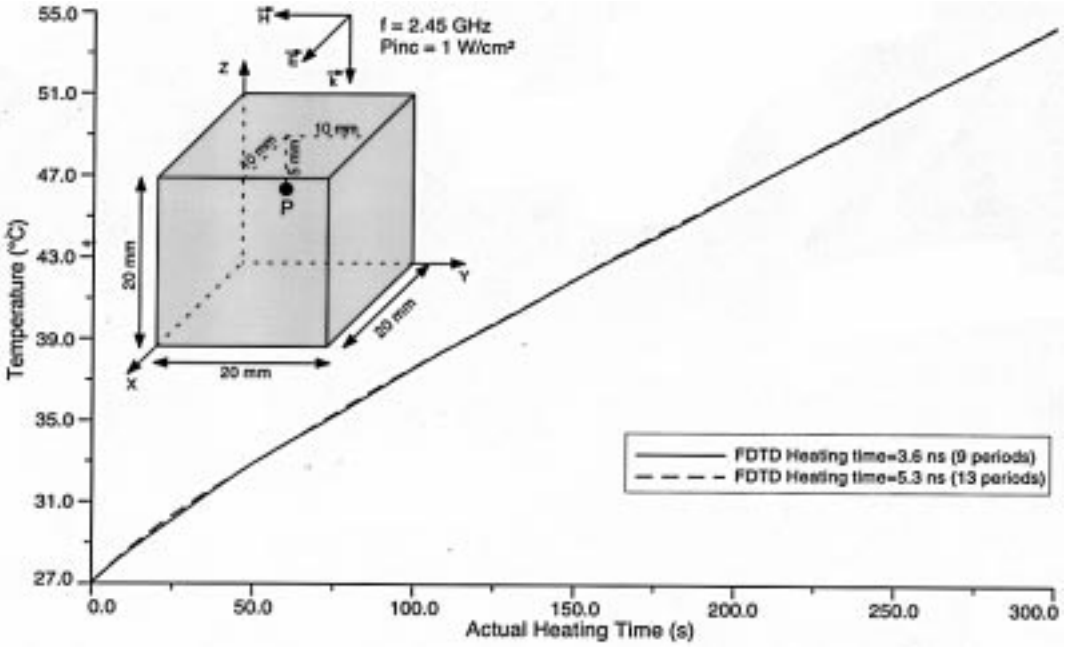

Fig. 3. Validation of the time-scaling procedure.

In addition to (20), convective boundary conditions can be used at the surfaces of the heated materials. Such conditions can be written as

$$\frac{\partial T}{\partial n} = \frac{h}{k_t}(T_{\text{ext}} - T_{\text{surf}}) \tag{28}$$

where

- k_t thermal conductivity of the material ($\text{W} \cdot \text{m}^{-1} \cdot \text{K}^{-1}$);
- h convection heat transfer parameter ($\text{W} \cdot \text{m}^{-2} \cdot \text{K}^{-1}$);
- n unit vector normal to the surface at the considered point;
- T_{surf} surface temperature of the material (K);
- T_{ext} temperature of the surrounding external medium (K).

This differential equation can be easily solved using the explicit FDTD scheme.

Rigorously, when (28) is used within a time-scaled procedure, it is necessary to multiply both the thermal conductivity k_t and the convection heat transfer parameter h by the scaling factor α. As only a ratio of these quantities appears in (28), α can be removed and the equation to solve remains unchanged.

Fig. 3 shows a three-dimensional (3-D) validation of this time scaling. The studied structure is a 20 × 20 × 20 mm water cube, illuminated by a plane wave at the microwave frequency of 2.45 GHz, and an incident power density of 1 W/cm^2. The cell size is 1 mm and the time step is 1.5 ps, and the medium is supposed to be temperature-dependent. Two FDTD computations were performed for two time windows of 4.5 and 6.1 ns, i.e., about 11 and 15 periods of the incident wave, but the heating processes were started only once the steady state is reached in the structure. Thus the FDTD heating durations are respectively reduced to 3.6 and 5.3 ns, while the actual heating duration T_{heat} is 300 s in all cases, with an initial temperature of 27 °C. The thermal properties of the medium are $C_m = 4180\ \text{J} \cdot \text{kg}^{-1} \cdot \text{K}^{-1}$, $\rho_m = 1000\ \text{kg} \cdot \text{m}^{-3}$ and $k_t = 0.55\ \text{W} \cdot \text{m}^{-1} \cdot \text{K}^{-1}$, leading to the thermal diffusivity $D_t = 131.58\ 10^{-9}\ \text{m}^2 \cdot \text{s}^{-1}$. This value was scaled to fit the computation windows according to (25), and results were scaled back to show the temperature evolution during the actual heating duration. The agreement between the curves is excellent, showing the validity of such a time scaling.

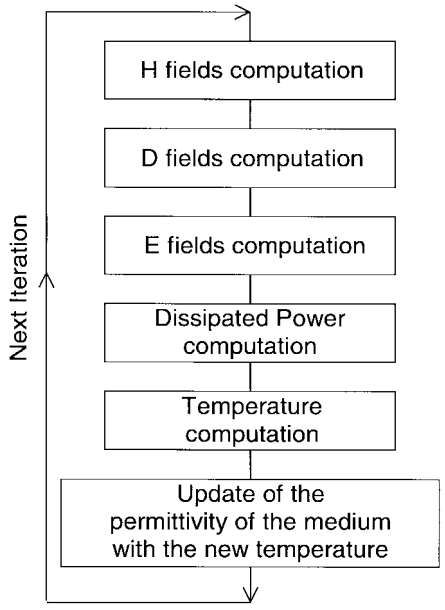

Fig. 4. Combined electromagnetic and thermal FDTD algorithm.

Moreover, several computations have been performed with this structure to see the influence of the scaling factor α on the results accuracy. It has been found that, even when the heating process is reduced to only 0.75 ns, leading to a large value of α ($\approx 10^{10}$), the relative error on the final temperature remains under 1%.

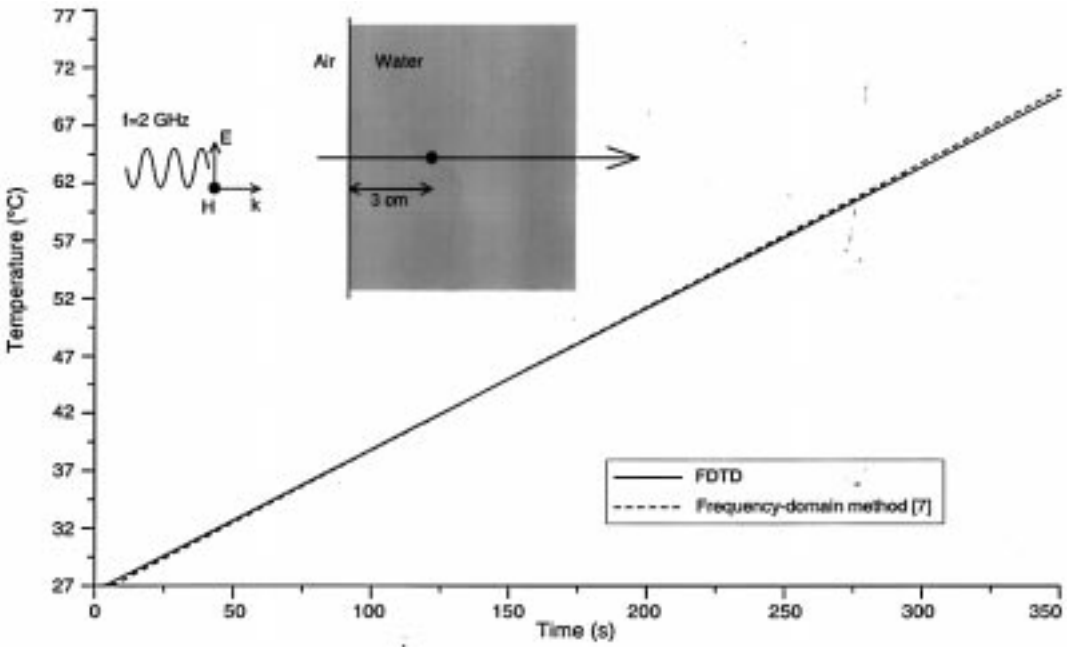

Fig. 5. Validation of the FDTD electromagnetic and thermal algorithm.

V. Applications

All quantities are now available to allow the three-dimensional determination of the electromagnetic fields, temperature distribution, and associated dielectric properties modifications within the same computation: as presented on Fig. 4, the electromagnetic fields are computed using the classical $(FD)^2TD$ scheme [22] for frequency-dependent materials. A knowledge of $\vec{E}$ and $\vec{D}$ allows us to calculate the instantaneous power dissipated per unit volume using the FDTD development of (16). Then the temperature is determined at the center of every FDTD cell containing the dissipative media at every time step, using the finite-difference expression of the heat transport equation (26). The temperature distribution is then used to update the static permittivity and relaxation time in each cell. It must be pointed out that since the temperature difference between two adjacent cells leads to different dielectric properties between neighboring cells, the heated materials become inhomogeneous, and this fact has to be considered for the computation of electric fields in every cell containing a dispersive medium.

In order to validate results obtained with the FDTD method, we have first studied the temperature evolution in water for the one-dimensional (1-D) configuration previously defined in Section III. The heating time of 350 s was scaled to the FDTD EM computation time, and the microwave frequency is 2 GHz. The results are compared with the solution obtained with a frequency-domain numerical method developed in [7], which uses the steady-state propagation equations to evaluate the power dissipated in the medium, assumed to be temperature-independent, and solves the heat transport equation (without time scaling) with an implicit finite-difference scheme. Thus, in our computations, the temperature variations did not affect the dielectric properties of the material. Shown in Fig. 5 is the comparison of the temperature evolution obtained at a point located 3 cm beneath the interface with our FDTD model and the frequential solution given by [7]. An excellent agreement is found between the two methods.

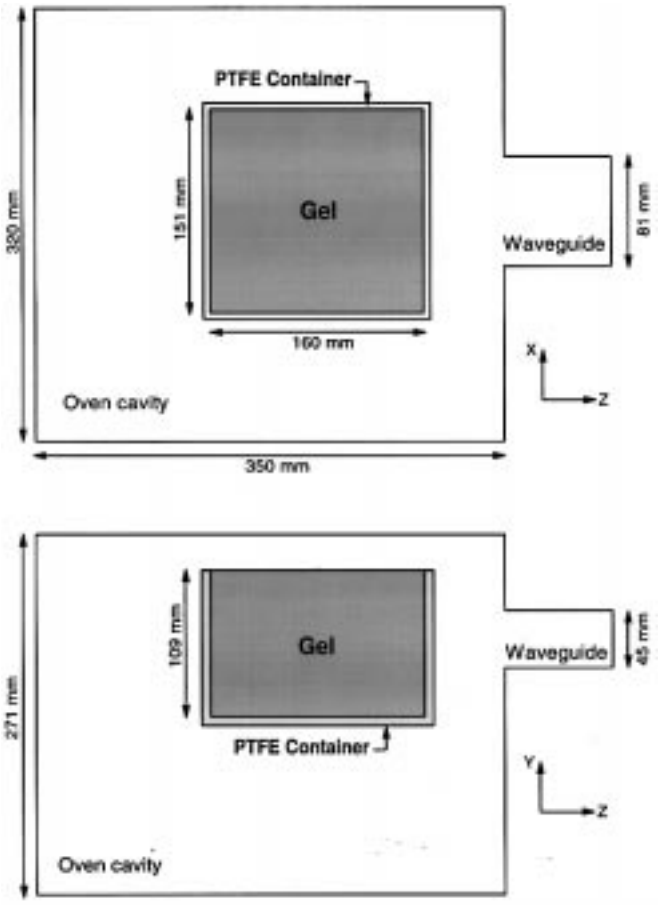

Fig. 6. Geometry of the studied microwave oven.

A more practical application is the heating process in a microwave oven. This three-dimensional problem has been extensively treated in [8], where the authors have successfully

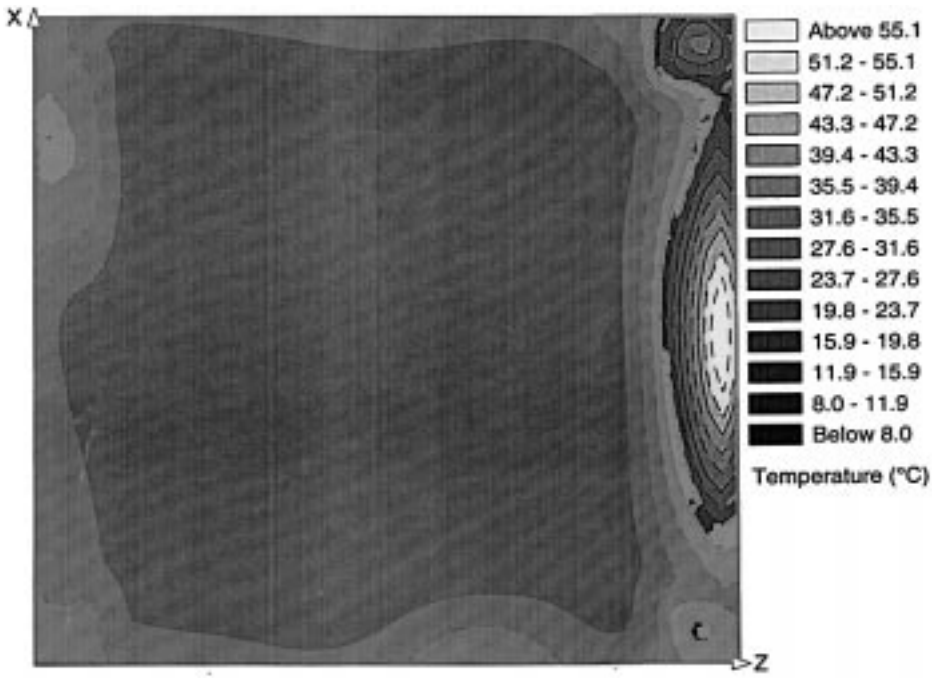

Fig. 7. Calculated temperature distribution in the workload at 180 s.

compared their numerical results with experimental measurements. In order to validate our method, we have performed 3-D FDTD computations considering the same geometry. The studied structure is presented on Fig. 6, and the FDTD mesh is the same as detailed in [8]. Energy at the working frequency of 2.45 GHz is supplied to the oven cavity through the waveguide, which is excited by a plane of equivalent electric and magnetic currents. The workload in the oven is a phantom food gel placed in a PTFE container. As far as we know, the dielectric properties of the gel were assumed to be frequency-independent in the FDTD computations presented in [8]. However, as the gel is mainly composed of water (66%), we assumed a Debye relaxation equation for the description of the dielectric properties of the gel. Concerning its temperature dependence, Ma *et al*. [8] used experimental data for the dielectric properties of the gel, and they interpolated the value of the complex permittivity for temperatures for which data were unavailable. From the experimental data given in [8], and assuming the same infinite permittivity as water ($\varepsilon_\infty = 5.5$), the values required by (7) and (8) have been computed to fit the measured data at best. Thus, the following values have been found:

$$W_a = 9.84 \cdot 10^{-21} \text{ J}$$
$$\tau_0 = 2.297 \cdot 10^{-12} \text{ s}$$
$$U = -1.77 \cdot 10^{-20} \text{ J} A_0 = 19.69.$$

The dielectric characteristics of the PTFE container are assumed to be independent of temperature and frequency, and the thermal properties of both gel and PTFE that we used are the same as in [8], i.e.,

$$D_t(\text{gel}) = 152.77 \cdot 10^{-9} \text{ m}^2 \cdot \text{s}^{-1}$$
$$k_t(\text{gel}) = 0.55 \text{ W} \cdot \text{m}^{-1} \cdot \text{K}^{-1}$$
$$D_t(\text{PTFE}) = 168.72 \cdot 10^{-9} \text{ m}^2 \cdot \text{s}^{-1}$$
$$k_t(\text{PTFE}) = 0.29 \text{ W} \cdot \text{m}^{-1} \cdot \text{K}^{-1}.$$

Moreover, a convective heat transfer coefficient of 10 $\text{W} \cdot \text{m}^{-2} \cdot \text{K}^{-1}$ was assumed to model a flow of air on the surface of the workload, due to the action of the oven fan. The air temperature in the oven cavity is 30 °C, while the initial temperature of the workload is 5 °C. The actual heating time is 180 s and has been scaled down to 12 ns (about 29 periods of the incident wave) for a total FDTD computation window of 15 ns (≈37 periods). The time required for this computation is quite reasonable, since only 70 min on a DEC Alpha/2100 Server (equivalent to 2 h and 40 min on an HP730 workstation) were necessary.

Fig. 7 presents the calculated temperature distribution in the workload at the end of the simulated heating time in the horizontal plane (XoZ). Taken from [8], Fig. 8 shows the experimental temperature distribution, obtained using a thermal imaging technique, for the same configuration (courtesy of Dr. C. Railton). It can be seen that the agreement between the two heating patterns is good, particularly concerning the location of the hot spots. Most of the heating takes place on the right face of the workload, the energy being supplied to the system at this point. It can also be noticed that the temperature has not been overestimated at the corners of the workload, showing the capability of the model to correctly handle the field variations at the interfaces between materials of different electrical properties.

VI. Conclusion

We have presented a complete 3-D (FDTD) [2] model allowing, within the same algorithm, to assess the temperature rise due to temperature-dependent dielectric losses. A realistic model of the temperature dependence of the Debye complex

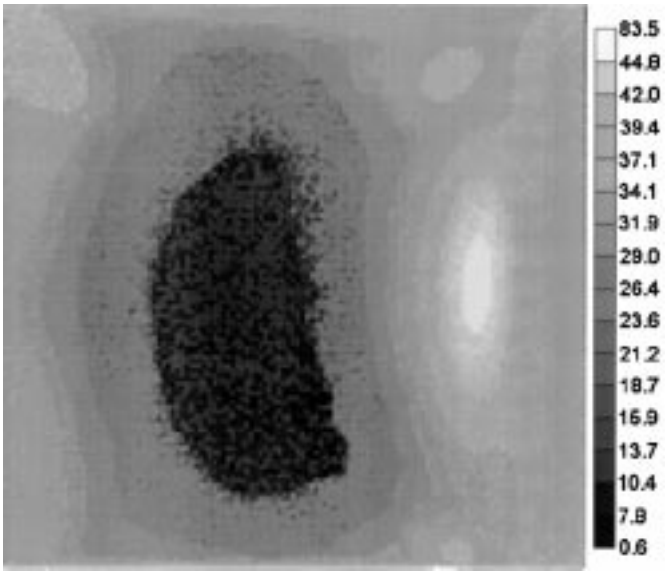

Fig. 8. Measured temperature distribution in the workload at 180 s (Courtesy of Dr. C. Railton [8]).

permittivity, used together with a time-domain expression of the dissipated power and a time-scaled formulation of the heat transfer equation, allows us to drastically reduce the computation times. The application to the heating phenomena in a microwave oven has shown, through good agreement between theory and experiment, the power of the method and its capability to model complex structures. The limitations of the model mainly lie in the fact that experimental data on the temperature dependence of the dielectric properties of materials are lacking. Another point to mention is that the conductivities of media and their related dissipated powers have not been taken into account, but work is currently in progress to develop analytical and numerical models of the temperature dependence of the materials conductivity.

ACKNOWLEDGMENT

The authors would like to thank Dr. C. Railton and his colleagues from the University of Bristol (U.K.) for permission to use and reproduce parts of their work.

REFERENCES

[1] J. M. Osepchuck, "A history of microwave heating applications," *IEEE Trans. Microwave Theory Tech.*, vol. MTT-32, pp. 1200–1224, Sept. 1984.
[2] A. R. Shapiro, R. F. Lutomirski, and H. T. Yura, "Induced fields and heating within a cranial structure irradiated by an electromagnetic plane wave," *IEEE Trans. Microwave Theory Tech.*, vol. MTT-19, pp. 187–196, Feb. 1971.
[3] A. Taflove and M. E. Brodwin, "Computation of the electromagnetic fields and induced temperatures within a model of the microwave-irradiated human eye," *IEEE Trans. Microwave Theory Tech.*, vol. MTT-23, pp. 888–896, Nov. 1975.
[4] M. K. Hessary and K. M. Chen, "EM local heating with HF electric fields," *IEEE Trans. Microwave Theory Tech.*, vol. MTT-32, pp. 569–576, June 1984.
[5] P. Y. Cresson, C. Michel, L. Dubois, M. Chive, and J. Pribetich, "Complete three-dimensional modeling of new microstrip-microslot applicators for microwave hyperthermia using the FDTD method," *IEEE Trans. Microwave Theory Tech.*, vol. 42, pp. 2657–2667, Dec. 1994.
[6] M. A. Stuchly and S. S. Stuchly, "Industrial, scientific, medical and domestic applications of microwaves," in *Proc. Inst. Elec. Eng.*, vol. 128, pt. A, no. 8, pp. 467–503. 1983.
[7] M. Nachman and G. Turgeon, "Heating pattern in multi-layered material exposed to microwaves," *IEEE Trans. Microwave Theory Tech.*, vol. MTT-32, pp. 547–552, May 1984.
[8] L. Ma, D.-L. Paul, N. Pothecary, C. Railton, J. Bows, L. Barratt, J. Mullin, and D. Simons, "Experimental validation of a combined electromagnetic and thermal FDTD model of a microwave heating process," *IEEE Trans. Microwave Theory Tech.*, vol. 43, pp. 2565–2572, Nov. 1995.
[9] M. Hamid, "Microwave drying of clothes," *J. Microw. Power Electromagn. Energy*, vol. 26, no. 2, pp. 107–114, 1991.
[10] J. C. Monzon, "Electromagnetic paper drying," *IEEE Trans. Microwave Theory Tech.*, vol. 43, pp. 299–305, Feb. 1995.
[11] P. L. Brian, "A finite-difference method of high-order accuracy for the solution of the three-dimensional transient heat conduction," *AIChE J.*, vol. 7, pp. 367–370, 1961.
[12] K. R. Foster, H. N. Kritikos, and H. P. Schwann, "Effect of surface cooling and blood flow on microwave heating of tissue," *IEEE Trans. Biomed. Eng.*, vol. BME-25, p. 313, 1978.
[13] J. F. Luy and J. Schmidl, "Temperature distribution in cylinder symmetric mm-wave devices," *IEEE Trans. Microwave Theory Tech.*, vol. 42, pp. 573–579, Apr. 1994.
[14] M. Sasaki, N. Yoshida, I. Fukai, and J. I. Fukuoka, "Analysis of the transient temperature distribution in a stripline with triple-layer dielectric," *IEEE Trans. Microwave Theory Tech.*, vol. MTT-24, pp. 119–121, Feb. 1976.
[15] R. J. Spiegel, "A review of numerical models for predicting the energy deposition and resultant thermal response of humans exposed to electromagnetic fields," (invited paper), *IEEE Trans. Microwave Theory Tech.*, vol. MTT-32, pp. 730–746, Aug. 1984.
[16] C. Q. Wang and O. P. Gandhi, "Numerical simulation of annular phased arrays for anatomically based models using the FDTD method," *IEEE Trans. Microwave Theory Tech.*, vol. 37, pp. 118–126, Jan. 1989.
[17] D. Sullivan, "Three dimensional computer simulation in deep regional hyperthermia using the finite-difference time-domain method," *IEEE Trans. Microwave Theory Tech.*, vol. 38, pp. 204–212, Feb. 1990.
[18] P. C. Cherry and M. F. Iskander, "FDTD analysis of power deposition patterns of an array of interstitial antennas for use in microwave hyperthermia," *IEEE Trans. Microwave Theory Tech.*, vol. 40, pp. 1692–1700, Aug. 1992.
[19] R. M. Joseph, S. C. Hagness, and A. Taflove, "Direct time integration of Maxwell's equations in linear dispersive media with absorption for scattering and propagation of femtosecond electromagnetic pulses," *Opt. Lett.*, vol. 16, no. 18, pp. 1412–1414, 1991.
[20] R. J. Luebbers, F. P. Hunsberger, K. S. Kunz, R. B. Standler, and M. Schneider, "A frequency-dependent finite-difference time-domain formulation for dispersive media," *IEEE Trans. Electromag. Compat.*, vol. 32, pp. 222–227, Aug. 1990.
[21] D. Sullivan, "A frequency-dependent FDTD method for biological applications," *IEEE Trans. Microwave Theory Tech.*, vol. 40, pp. 532–539, mar. 1992.
[22] O. P. Gandhi, B. Q. Gao, and J. Y. Chen, "A frequency-dependent finite-difference time-domain formulation for general dispersive media," *IEEE Trans. Microwave Theory Tech.*, vol. 41, pp. 658–665, Apr. 1993.
[23] P. Debye, *Polar Molecules*. New York: Dover, 1945.
[24] R. H. Cole, "Theories of dielectric polarization and relaxation," in *Progress in Dielectrics*, J. Birks and J. Hart, Eds. London, U.K: Heywood, 1961, vol. 3.
[25] H. Fröhlich, *Theory of Dielectrics*. Oxford: Clarendon, 1949, ch. II.
[26] R. W. P. King and G. S. Smith, *Antennas in Matter*.Cambridge, MA: MIT Press, 1981, ch. 6.
[27] K. S. Cole and R. H. Cole, "Dispersion and absorption in dielectrics," *J. Chem. Phys.*, vol. 9, pp. 341–351, Apr. 1941.
[28] J. G. Kirkwood, "The dielectric polarization of polar liquids," *J. Chem. Phys.*, vol. 7, pp. 911–919, Oct. 1939.
[29] H. A. Lorentz, *Theory of Electrons*. New York: Dover, 1952.
[30] B. K. P. Scaife, *Principle of Dielectrics*. New York: Oxford, 1989, ch. 3.
[31] R. J. Meakins, "Mechanisms of dielectric absorption in solids" in *Progress in Dielectrics*, J. Birks and J. Hart, Eds. London, UK: Heywood, 1961, vol. 3.
[32] A. Von Hippel, "Structure and dielectric response of molecules" in *Dielectrics Materials and Applications*, A. Von Hippel, Ed. Cambridge, MA: MIT Press, 1954.
[33] A. Taflove and M. E. Brodwin, "Numerical solution of steady-state electromagnetic scattering problems using the time-dependent Maxwell's equations," *IEEE Trans. Microwave Theory Tech.*, vol. MTT-23, pp. 623–630, Aug. 1975.

François Torres was born in Limoges, France, in 1963. He received the Ph.D. degree from the University of Limoges in 1991.

Since 1986, he has been with the Electromagnetic Team of the Institut de Recherche en Communications Optiques et Microondes (I.R.C.O.M.), U.R.A., Centre National de la Recherche Scientifique (C.N.R.S.), 356. He became a Researcher in 1993. His current areas of research include electromagnetic modeling of materials, electromagnetic compatibility (EMC), microstrip antennas, high-power microwaves, and electromagnetic topology.

Bernard Jecko was born in Trelissac, France, on May 18, 1944. He received the grade of es science physic Doctor in electronics from the University of Limoges, Limoges, France, in 1979.

He is now a Professor at the University of Limoges and manages the Electromagnetic Research Team in the Microwave and Optic Communication Institute (I.R.C.O.M.). His main interest is in studying scattering problems of electromagnetic waves, particularly in the time domain.